JOURNAL
OF THE AMERICAN CHEMICAL SOCIETY

VOLUME 102, NUMBER 10 MAY 7, 1980

Structure and Properties of Liquid Ammonia[1]

William L. Jorgensen*[2] and Mustafa Ibrahim

Contribution from the Department of Chemistry, Purdue University, West Lafayette, Indiana 47907. *Received August 9, 1979*

Abstract: An intermolecular potential function for the ammonia dimer has been obtained from ab initio molecular orbital calculations with a minimal basis set. Dimerization energies for 250 orientiations of $(NH_3)_2$ selected using the iterative energy distributed random geometries method were fit to a 12-6-3-1 potential with standard deviations of 0.2–0.3 kcal/mol. The predicted dimerization energy from the potential function is −3.6 kcal/mol. This function and a scaled version yielding a dimerization energy of −4.5 kcal/mol have been used in Monte Carlo simulations of liquid ammonia at its boiling point (−33.35 °C). Detailed structural and energetic results have been obtained and are compared with experimental data. The radial distribution functions are not altered significantly by scaling the potential; however, the energy is brought into good agreement with experiment, particularly when three-body effects are considered. The calculated NN radial distribution functions are in better agreement with X-ray results than from earlier molecular dynamics simulations; however, the experimental data are still more structured. Liquid ammonia is predicted to bear little resemblance to the solid. Stereoplots reveal short polymeric chains in the liquid. Although the first peak in g_{NN} yields a coordination number of 12 in accord with experiment, most monomers are in only one or two hydrogen bonds and there is 5–10% free monomer present. Roughly linear hydrogen bonding predominates.

I. Introduction

Hydrogen bonding has been examined relentlessly owing to the ubiquity and utility of polar protic solvents, the challenge of developing theories to describe the properties of nonideal gases and liquids, and in view of the importance of hydrogen bonding in determining the structures and reactivities of biomolecules. The advent of computer simulation techniques has provided the possibility of obtaining detailed structural and energetic descriptions of complex liquids at the molecular level. The applicability of such computations to modeling hydrogen-bonded liquids has been established by recent molecular dynamics and Monte Carlo statistical mechanics calculations for water,[3] hydrogen fluoride,[4] and methanol.[5] Preliminary molecular dynamics studies of liquid ammonia[6a] poorly reproduced the NN radial distribution function which has been determined by X-ray diffraction.[7] Modifications to the original potential function provided only modest improvement;[6b] however, a new function based on virial coefficient and solid-phase data appears promising.[6c]

In our studies, intermolecular potential functions have been obtained from ab initio molecular orbital calculations on the appropriate dimers. This approach was pioneered by Clementi and co-workers;[8] however, significant advances have been made in the procedures used to select the orientations of the dimers.[3e,4b,5a] The advantage of the quantum-mechanical route is apparent from the shortage of accurate experimental data on the structures and energetics of gas-phase dimers which hinders the empirical construction of intermolecular potential functions. A complication is that the results depend on the choice of basis sets and correlation-energy corrections. This problem has been thoroughly explored for water. The quality of the results for the liquid is not found to improve smoothly as the ab initio calculations become more sophisticated. In fact, potential functions derived from minimal basis set[3e] and large basis set plus configuration interaction (CI)[8b] calculations yield similar structural and thermodynamic results for liquid water.[3b-e] Intermediate levels of ab initio calculations are less successful owing primarily to their poorer estimates of hydrogen-bond energies.[3c,e]

More recently, potential functions based on minimal basis set calculations have provided reasonable descriptions of liquid hydrogen fluoride and methanol in Monte Carlo simulations.[4b,5] In the latter case, dispersion corrections were necessary particularly for the interactions between the methyl groups. To extend our studies of hydrogen-bonded solvents of importance in organic chemistry, the approach has been applied to liquid ammonia as presented here.

To begin, an intermolecular potential function is derived from minimal basis set (STO-3G) calculations on 250 orientations of the ammonia dimer selected using the iterative energy distributed random geometries procedure. An excellent fit of the computed dimerization energies to a 12-6-3-1 potential function is obtained. A Monte Carlo simulation of the liquid at its boiling point (−33.35 °C) is reported using the potential. The resultant NN radial distribution function is in significantly better agreement with experiment than the earlier molecular dynamics results.[6a,b] However, the computed energy is too high. This deficiency is overcome by scaling the potential function. The scaling has little effect on the radial distribution functions. A thorough environmental analysis is presented including stereoviews of configurations of the liquid and hydrogen-bonding and energy distributions. In contrast to the structure of the solid, short polymeric chains are apparent in the liquid and most monomers are in only one or two hydrogen bonds. It is further established that minimal basis set calculations can be used to provide useful, preliminary intermolecular potential functions for hydrogen-bonded dimers with no or minor modifications.

0002-7863/80/1502-3309$01.00/0

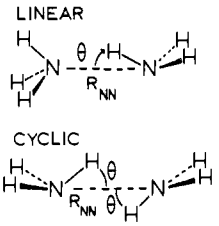

Figure 1. Definition of geometric variables for the linear and cyclic ammonia dimers.

II. The 12-6-3-1 Potential Function

A. The Fitting Procedure. The ammonia monomers have been held rigid in their experimental microwave geometries (r(NH) = 1.0124 Å, ∠HNH = 106.67°)[9a] in all aspects of this work. The iterative energy distributed random geometries (IEDRG) method was used to select the dimer geometries for the ab initio calculations.[3e,5a] To begin, 50 orientations of the dimer were chosen near interesting portions of the potential surface, particularly around the minima for the linear and cyclic forms of the dimer (Figure 1) and in various repulsive configurations. Dimerization energies were computed with the minimal STO-3G basis set using the GAUSSIAN/74 program[10] on the CDC/6500-6600 system at Purdue University.

The dimerization energies were fit to a 12-6-3-1 potential

$$\Delta E(12\text{-}6\text{-}3\text{-}1) = \sum_{i<j}^{\text{charges}} \frac{q_i q_j}{r_{ij}} + \sum_{\mu<\nu}^{\text{atoms}} \left(\frac{b_{mn}}{r_{\mu\nu}^{3}} + \frac{c_{mn}}{r_{\mu\nu}^{6}} + \frac{d_{mn}}{r_{\mu\nu}^{12}} \right)$$

as for water[3e] and hydrogen fluoride.[4a,b] A five-particle model was used to represent a monomer consisting of the four atoms and a dummy particle placed on the C_3 axis in the position of a lone pair. Charges of $+Q$ were placed on each hydrogen and $-3Q$ on the pseudo-lone pair. The interactions between the intermolecular pairs of point charges determine the Coulombic part of the potential. The short-range forces are contained in the second sum over intermolecular pairs of atoms with types m and n. The charge Q and the N to pseudo-lone pair distance are two adjustable parameters and there is a b, c, and d for NN, NH, and HH interactions. As discussed previously, it is necessary to restrict the r^{-3} terms so they cancel at large r.[11] This condition is met by taking $b_{NH} = -\frac{1}{6}(b_{NN} + 9b_{HH})$. Therefore, the total number of adjustable parameters is ten.

The potential obtained from fitting the dimerization energies for the first 50 points was used with a program that randomly generates dimer geometries in all orientations to produce 25 new geometries with predicted dimerization energies evenly covering the range −4.0 to 4.0 kcal/mol. STO-3G dimerization energies were computed for these points and a new fit was made to the expanded data base of 75 points. The new potential was used to create 25 more geometries and the iterative procedure was repeated until 250 geometries were processed. The 12-6-3-1 function was essentially unchanged after 175 points.

The fit for points with low energy is enhanced by using a weighting function $\omega_i = 1 + \alpha \exp[-(\Delta E_i - \Delta E_0)/kT]$ in the least-squares procedure. ΔE_0, kT, and α were set at −6.0 kcal/mol, 0.6 kcal/mol, and 100. Increasing α beyond this point yielded too much deterioration in the high-energy fit. The final parameter values are given in Table I. As always, physical significance should not be attributed to individual parameter values since they are coupled and not necessarily unique. The standard deviations for the fit to the 250 points are $\sigma_{<6}$ (0.29), $\sigma_{<0}$ (0.21), $\sigma_{<-1}$ (0.24), and $\sigma_{<-3}$ (0.20) where $\sigma_{<\chi}$ refers to the deviation in kcal/mol for all points with dimerization energies below χ kcal/mol. This is the best fit that we have obtained for any quantum-mechanical potential to date.

The predictions for dimerization energies from the STO-3G calculations and 12-6-3-1 potential are compared for the 250 points in Figure 2. The effect of the weighting function is apparent in the figure. The even distribution of points over the range is due to the IEDRG procedure.

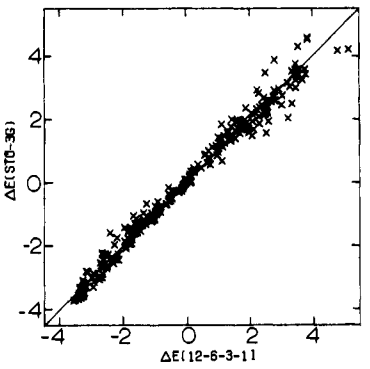

Figure 2. Comparison of dimerization energies (kcal/mol) for ammonia from STO-3G calculations and the 12-6-3-1 potential function.

Table I. Parameters for the 12-6-3-1 Potential Function for $(NH_3)_2$ Fit to STO-3G Dimerization Energies[a]

	parameter		
	NN	NH	HH
b	344.0825	(−102.2190)[b]	29.914 61
c	−1709.910	97.93475	30.035 97
d	1 235 070.	968.1959	351.8337
	q_L	q_H	r(NL)
	−4.025 829	(1.341 943)[b]	0.870 520 7

[a] All values correspond to energies in kcal/mol and distances in Å. L is a point charge placed on the C_3 axis at a distance r(NL) from nitrogen away from the hydrogens. [b] Values determined by symmetry (see text).

B. Geometry Optimizations. Optimizations for the linear and cyclic dimers were carried out with STO-3G calculations and the 12-6-3-1 potential with the monomers rigid. Not surprisingly, the results in Table II are very similar. Recent gas-phase measurements also favor a linear rather than cyclic structure for the dimer.[9c] The quality of the fit is further demonstrated in Figures 3 and 4. The plots illustrate the effects on the energy for the linear dimer of varying R_{NN} and θ, with θ and R_{NN} fixed at their optimum values in Figures 3 and 4, respectively.

The hydrogen bond in the linear dimer is predicted to be slightly bent with a dimerization energy of −3.6 kcal/mol. Including d orbitals on the nitrogens with the 6-31G* basis set raises the dimerization energy to −2.9 kcal/mol.[12] More advanced calculations do not appear to have been reported. Experimentally, dimerization *enthalpies* of −4.5 ± 0.4 and −4.4 kcal/mol have been obtained from IR and virial coefficient data, respectively.[13] Applying the classical correction[5a] of $2RT$ at 25 °C to these values gives a ΔE_{el} of ca. −5.6 kcal/mol for comparison with the theoretical values. The experimental numbers seem too low because all theoretical results predict a significantly lower dimerization energy for water than ammonia. However, recent thermal conductivity data have established ΔE_{el} for the water dimer to be −5.44 ± 0.7 kcal/mol, in good agreement with the best theoretical estimates.[14] It seems unlikely that ΔE_{el} for the ammonia dimer should be below −4.5 kcal/mol, implying a lower limit of about −3.5 kcal/mol for the enthalpy change at 25 °C. Clearly, further theoretical and experimental investigations are warranted.

As usual, the STO-3G intermolecular separation for the dimer is probably 10% too short, while the 6-31G* value is an overestimate.[12] The NN distance in solid ammonia at −102 °C is 3.38 Å[15] and the first peak in g_{NN} for the liquid at 4 °C occurs at 3.37 Å.[7] So, as before,[3e,4b] the 12-6-3-1 potential is anticipated to shift the peaks in the radial distribution functions

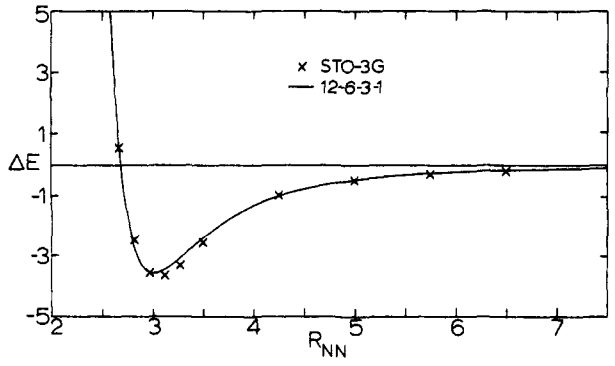

Figure 3. Variation of the dimerization energy (kcal/mol) for the linear ammonia dimer with NN separation (Å) from STO-3G calculations and the 12-6-3-1 potential function. The angle θ is fixed at its optimum value for the minimum in both cases.

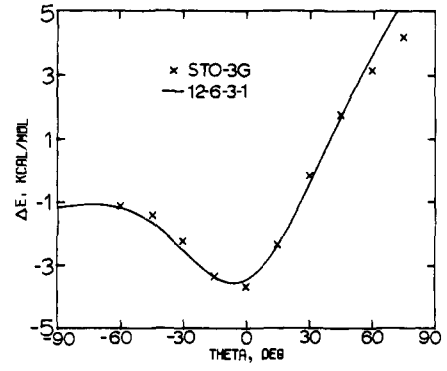

Figure 4. Variation of the dimerization energy (kcal/mol) for the linear ammonia dimer with angle θ (deg) from STO-3G calculations and the 12-6-3-1 potential function. R_{NN} is fixed at its optimum value for the minimum in both cases.

Table II. Optimized Geometries and Dimerization Energies for $(NH_3)_2$[a]

	R_{NN}, Å	θ, deg	$-\Delta E$, kcal/mol
	Linear Dimer		
STO-3G	3.067	−4.1	3.74
12-6-3-1	3.011	−6.1	3.56
6-31G*	3.44[b]	0.0[b]	2.9[b]
	Cyclic Dimer		
STO-3G	3.252	43.2	1.63
12-6-3-1	3.197	43.9	1.60

[a] Geometric variables are defined in Figure 1. The experimental geometries for the monomers (ref 9) have been used in the STO-3G and 12-6-3-1 calculations. [b] Reference 12.

for the liquid to shorter distances by about 0.2 Å after the effect of temperature is included.

III. Monte Carlo Simulations

Monte Carlo statistical mechanics simulations were executed for liquid ammonia using the 12-6-3-1 potential. As discussed below, the computed potential energy (−3.20 kcal/mol) is about 2 kcal/mol above the experimental value. In view of the importance of three-body effects in hydrogen-bonded liquids (vide infra), a reasonable tactic in the two-body format is to construct an effective potential that yields acceptable agreement with experimental data for the liquids. This approach was adopted by Rahman and Stillinger in their seminal studies on water.[3a] In this spirit, a scaled version of the potential termed S-12-6-3-1 was also used in a Monte Carlo calculation to improve the energy. The scaling factor was taken as 1.264 76 to yield a minimum dimerization energy of −4.5 kcal/mol, which is at the lower limit discussed above. A further rationale for the choice comes from an analysis of dipole moments. Although the r^{-1} and r^{-3} terms in the 12-6-3-1 potential are not independent, the charges and R_{NL} can be used to provide an estimate of 1.33 D for the dipole moment of a monomer. The scaling increases the value to 1.49 D, which compares well with the experimental number, 1.47 D.[16] Results from both simulations are presented below.

The Monte Carlo calculations were run at the boiling point (−33.35 °C)[17,18] of the liquid since this is the typical condition for performing organic reactions in the solvent. The experimental density (0.682 g/cm^3)[17] was used for cubic samples of 128 molecules (640 particles). Consequently, an edge of the cube was 17.4435 Å long. The calculations were carried out in the standard manner using periodic boundary conditions and the Metropolis sampling algorithm. Details of such simulations may be found elsewhere.[4a] The energy of a configuration was computed from the pairwise sum of the dimerization energies, as usual.

$$E_i = \sum_{a<b} \Delta E_{ab}$$

The neglect of higher order terms in the series is of concern for hydrogen-bonded liquids. For water, the influence of three-body and higher order effects has been estimated from ab initio calculations on trimers and from simulations of the liquid to lower the energy of the liquid by 1–2 kcal/mol or roughly 15%.[3] From minimal and double ζ basis set calculations on ammonia trimers[19] and considering the computed structure of the liquid (vide infra), the cooperative effect in ammonia is anticipated to account for 0.5–1.0 kcal/mol of the energy, which is still about 15%.

A spherical cutoff at an NN separation of 8.0 Å was used in evaluating the potential functions. As usual in Monte Carlo simulations, corrections were not made for interactions with molecules beyond the cutoff. Including this effect has been estimated to lower the energy of water by 0.15 kcal/mol for a sample of 64 molecules.[3d] This is insignificant in view of the statistical fluctuations in the calculations, the neglect of three-body interactions, and the nature of the potential functions. The larger sample sizes and weaker interactions in the present simulations should also nearly eliminate the effect.

A move to create a new configuration consisted of picking a molecule, translating it in all three Cartesian directions, and rotating it about an axis. Each step of this procedure was performed randomly. The ranges for the translations and rotations were ±0.15 Å and ±15°, which provided acceptance rates of roughly 50% for new configurations. The simulations were initiated with the monomers evenly distributed and hydrogen bonded in the periodic cube. Each run consisted of 500 000–600 000 attempted moves. Control functions demonstrated that equilibrium was achieved after 200 000–250 000 attempted moves. Averaging for properties and distribution functions was only performed over the final 300 000 configurations. By analogy to results for water,[20] the length of the present runs may lead to errors of about 1% for the computed energies and 3% for the radial distribution functions. The heat capacity converges much more slowly and may be in error by 20%.[20]

IV. Results and Discussion

A. Thermodynamics. Calculated and experimental values for thermodynamic quantities are compared in Table III. The energy (E) and heat capacity include corrections of $3RT$ and $3R$ for the classical kinetic energy of rotation and translation of the monomers. The internal potential energy of the liquid, E_i, is calculated directly in the simulations. It may be equated with the energy of vaporization of the liquid going to the ideal gas, $\Delta E°_{vap}$, assuming that the kinetic energy of the liquid and ideal gas are the same. Unfortunately, $\Delta E°_{vap}$ is rarely re-

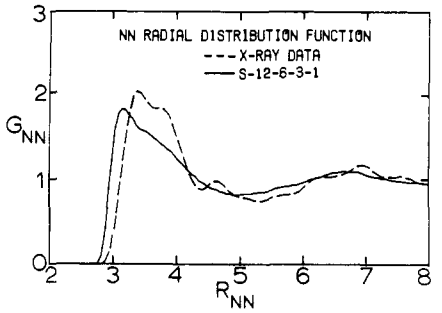

Figure 5. NN radial distribution functions for liquid ammonia obtained from the S-12-6-3-1 potential function at −33.35 °C and from X-ray data at +4 °C (ref 7). Distances are in Å throughout.

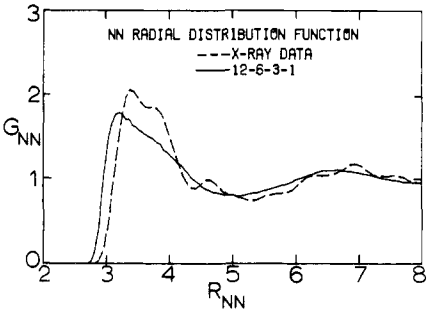

Figure 6. NN radial distribution functions for liquid ammonia obtained from the 12-6-3-1 potential function at −33.35 °C and from X-ray data at +4 °C (ref 7).

Table III. Thermodynamic Properties for Liquid Ammonia at −33.35 °C.[a]

	calcd		
	12-6-3-1	S-12-6-3-1	exptl
$-E_i$	3.20	4.48	5.18[b]
$-E$	1.77	3.05	3.75,[a,b] 3.72[c]
$\Delta H°_{vap}$	3.67	4.95	5.66[b]
ΔH_{vap}	3.60	4.88	5.58[c]
C_v	12.7	13.3	12.7[c]

[a] Energies in kcal/mol; C_v in cal/mol·K. E_i is the internal potential energy. E and C_v include the classical kinetic energy contributions. [b] Calculated from virial-coefficient data; see text. [c] Reference 18.

ported experimentally; however, ΔH_{vap} is known for ammonia.[18]

$$\Delta E°_{vap} = \Delta H°_{vap} - P\Delta V°$$

$$\Delta H°_{vap} = \Delta H_{vap} + (H° - H)$$

$\Delta E°_{vap}$ can be obtained from ΔH_{vap} if a correction for the nonideality of the gas can be made. Using the virial equation of state for the gas, the departure function $(H° - H)$ can be derived as

$$H° - H = \frac{RT}{V}\left(T\frac{dB}{dT} - B\right)$$

where B is the second virial coefficient. Virial-coefficient data for ammonia[13b,21] have been obtained and may be expressed in the form

$$B(T) = \alpha - \beta T^{-1} \exp(\gamma T^{-2})$$

Using the parameters of Keyes,[21a] which are for 238–598 K, $H° - H$ is then 0.076 kcal/mol at the boiling point. Similarly, small enthalpy differences are found for water and methanol at 25 °C; however, hydrogen fluoride vapor is much more associated.[3-5] The correction has been applied to yield the experimental data for $\Delta H°_{vap}$, E_i, and E and the theoretical value for ΔH_{vap} in Table III.

The scaled potential provides a good estimate of the energy of liquid ammonia in view of the neglect of three-body effects which could primarily account for the remaining 0.7 kcal/mol. This may be considered as support for a dimerization energy of about −4.5 kcal/mol for the gas-phase dimer.

The experimental C_v and C_p for liquid ammonia are 12.7 and 18.0 cal/mol·deg at the boiling point.[18] In contrast, for water at 25 °C, C_p and C_v are nearly identical owing to the liquid's unusually small coefficient of expansivity. The computed values of C_v for ammonia are in excellent agreement with experiment. However, the inclusion of three-body corrections should raise the computed values somewhat. The slow convergence of heat capacities in Monte Carlo simulations must also be recalled.[20,22]

B. Radial Distribution Functions. Radial distribution functions, $g_{xy}(r)$, are related to the probability or occurrence of atoms with type y at a distance r from atoms of type x in the liquid. They are computed from

$$g_{xy}(r) = \frac{\langle N_y(r, r + dr)\rangle}{\rho_y 4\pi r^2 dr}$$

where the numerator is the average number of y atoms in the shell between r and $r + dr$. The denominator normalizes the distribution so that $g_{xy} = 1$ when N_y does not deviate from the average density for the liquid, ρ_y. Peaks in $g(r)$ are often assigned to solvation shells or other intermolecular structural features in liquid.

The results for g_{NN} from the two simulations at −33.35 °C are compared with the X-ray data obtained by Narten at 4 °C in Figures 5 and 6. Although the effect on the energy was substantial, the scaling makes almost no statistically significant changes in the radial distribution functions. The broad first band is slightly sharper and the shoulder at 3.6 Å more distinct with the scaled potential. The height of the maximum is 1.84 at 3.16 Å, while the experimental value is 2.06 at 3.37 Å. The first peak from the simulations could easily be decomposed into two bands as suggested by the pronounced shoulder in the experimental curve at 3.7 Å. The small feature at 4.6 Å in the X-ray data is reminiscent of the ripple at 3.8 Å for liquid water.[3,23] Neither peak has been reproduced in theoretical studies. The calculated distribution functions for ammonia clearly show a second band centered at 6.7 Å; however, it is not as structured as the experimental results. Some further enhancement to the structure would be expected for experimental data at −33 °C. The peaks from the simulations are shifted to shorter NN separations by about 0.2 Å in comparison to the experimental data, as anticipated above.

Integrating the first peak in g_{NN} to its minimum at 5.1 Å for the 12-6-3-1 potential and at 4.9 Å for the scaled function reveals 12.9 and 11.5 neighbors, respectively. The experimental figure is 12 at 5 Å which is consistent since the cutoff limit is somewhat arbitrary. Overall, the theoretical and experimental radial distribution functions are in rough accord. Significant improvement has been made over the early molecular dynamics data which gave a height of 3–4 for the first peak in g_{NN}.[6a,b]

To obtain some indication of possible errors in the computed pressure, the total density fluctuation, $\Delta\rho(r)$, may be plotted.[4b,5b] The function gives the difference

$$\Delta\rho(R) = 1 + \int_0^R 4\pi\rho r^2 g(r)\, dr - 4/3\pi R^3\rho$$

in the number of neighbors calculated from a radial distribution function and that expected assuming uniform density. The results from the S-12-6-3-1 potential and Narten's data are compared in Figure 7 using g_{NN}. It is apparent that the integrals of the distribution functions are similar. No serious error in the pressure for the simulations is anticipated.

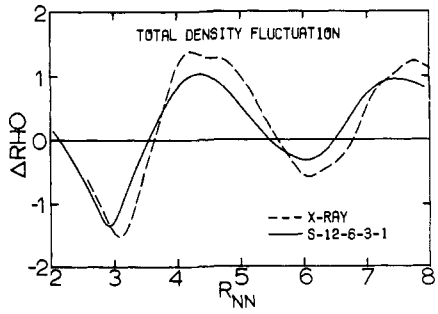

Figure 7. The total density fluctuations computed from the NN radial distribution functions.

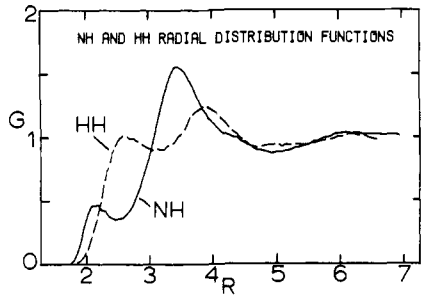

Figure 8. NH and HH radial distribution functions for liquid ammonia obtained from the S-12-6-3-1 potential function at −33.35 °C.

The NH and HH radial distribution functions computed from the scaled potential are shown in Figure 8. The results from the 12-6-3-1 function are essentially identical. No experimental guide is available in this case since the necessary neutron-diffraction data have not yet been reported. The most intriguing feature is the small peak at 2.2 Å that may be assigned to a hydrogen-bonded hydrogen at an NN separation of 3.2 Å assuming a linear hydrogen bond. The peak integrates to 1.07 hydrogens, which suggests that the monomers in the liquid are in an average of about two hydrogen bonds each. In contrast, the novel structure of the solid has six hydrogen bonds per monomer, three as proton donor and three as acceptor.[15] A thorough analysis of the hydrogen bonding is presented below.

C. Energy Distribution Functions. The distributions of binding energies calculated for the monomers in the liquid are shown in Figure 9. The monomers experience a spectrum of energetic environments covering a 15 kcal/mol range. Naturally, the distribution from the scaled potential is centered at lower energy. The curves are unimodal, which is consistent with a "continuum" model for the liquid.

The distributions of dimerization energies for a monomer in the liquid are displayed in Figure 10. The ordinate gives the average number of molecules that interact with a monomer with the dimerization energy shown on the abscissa. The minima for the linear dimer from the 12-6-3-1 and S-12-6-3-1 potentials restrict the dimerization energies to be above −3.6 and −4.5 kcal/mol. Also, most interactions involve distant molecules and appear in the spike between ±1 kcal/mol. The shoulders at low energy are attributed to hydrogen-bonded neighbors. The bands are not as well defined as for water, hydrogen fluoride, and methanol, which have definite minima between −2.0 and −2.5 kcal/mol.[3e,4b,5b] Rough deconvolutions of the shoulders suggest hydrogen-bonding limits of −2.0 kcal/mol for the S-12-6-3-1 potential and −1.6 kcal/mol for the 12-6-3-1 function. Integration to these values predicts 1.8 and 1.5 hydrogen-bonded neighbors per monomer for the scaled and unscaled potentials, respectively. This agrees with the estimates from the NH radial distribution functions in view of the arbitrariness of the integration limits.

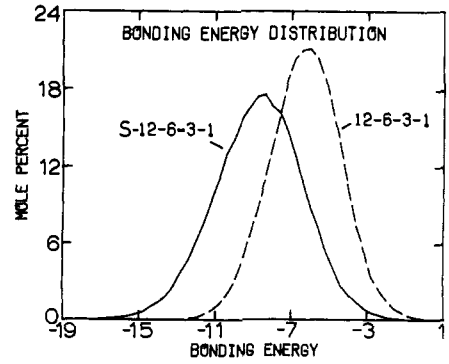

Figure 9. Distributions of total bonding energies (kcal/mol) for the monomers in liquid ammonia from the two Monte Carlo simulations. The units for the Y-axis are mol % per kcal/mol.

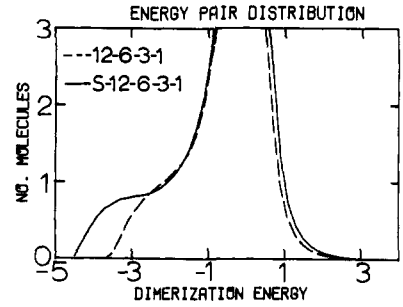

Figure 10. Distributions of dimerization energies (kcal/mol) for a monomer in liquid ammonia. The units for the *Y* axis are molecules per kcal/mol.

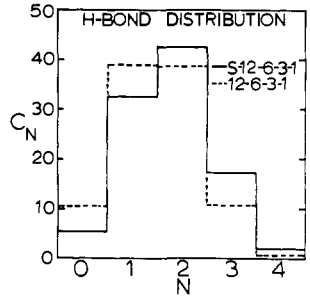

Figure 11. Distributions of coordination numbers for hydrogen-bonded neighbors from the two Monte Carlo simulations. The units for the *Y* axis are mole percent. A hydrogen bond is defined by a dimerization energy below −2.0 kcal/mol for the S-12-6-3-1 potential and below −1.6 kcal/mol for the 12-6-3-1 potential.

D. Hydrogen-Bond Distributions. Configurations were stored every 2000 attempted moves during the Monte Carlo runs. After the hydrogen-bonding limits were established from the energy pair distributions, the saved configurations were analyzed to obtain detailed insights into the hydrogen bonding.

The distributions of hydrogen-bond numbers are shown in Figure 11. Most monomers (ca. 75%) share one or two hydrogen bonds, while about 15% are in three hydrogen bonds and there is 5–10% free monomer present in the liquid. These distributions are consistent with polymeric chains in the liquid as were found for hydrogen fluoride[4b] and methanol.[5b] Stereoplots of configurations of the periodic cube confirm the proposal for ammonia. Typical configurations from the simulations with the S-12-6-3-1 and 12-6-3-1 functions are displayed in Figures 12 and 13. In viewing the plots, it must be remembered that monomers on one side of the cube also interact with monomers on the opposite face.

The darkened nitrogens in Figure 12 point out a chain with at least six or seven hydrogen-bonded monomers. The chains are highly bent; however, the hydrogen bonding appears

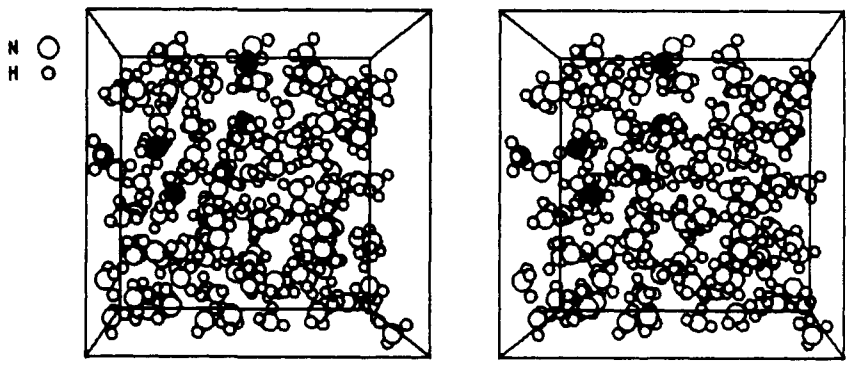

Figure 12. Stereoplot of a configuration from the simulation of liquid ammonia with the S-12-6-3-1 potential function. The blackened nitrogens point out a hydrogen-bonded chain.

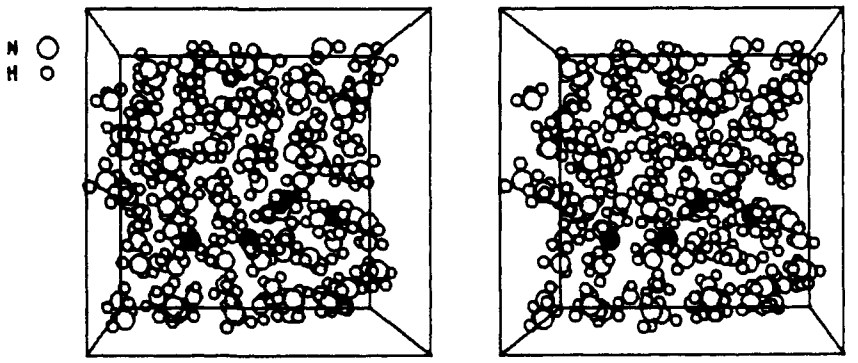

Figure 13. Stereoplot of a configuration from the simulation of liquid ammonia with the 12-6-3-1 potential function. A central monomer in the darkened tetramer is acting as a double hydrogen bond donor.

roughly linear. Many short chains and dimers are apparent. The tetramer highlighted in Figure 13 is worthy of note because a central monomer is acting as a double hydrogen bond donor. Cyclic polymers are not evident in the plots.

The explanation of the coordination-number distributions is then straightforward. The monomers in one hydrogen bond occur at chain ends and in dimers. The monomers in two and three hydrogen bonds are interior to chains and at branch points (Y junctions) of the chains. As noted before, the structure of the solid is very different.[15] Some additional support for this prediction can be found from thermodynamic data. The structures of solid and liquid methanol are both dominated by hydrogen-bonded chains so the heat of fusion is relatively small (0.77 kcal/mol).[5] However, since the vapor is only slightly associated, the heat of vaporization is large (8.42 kcal/mol). For ammonia, the two values are closer, 1.35 and 5.58 kcal/mol. Thus, for ammonia the disorder upon melting is a much larger fraction of the increase in disorder upon vaporization. The ratios of the heats of fusion to heats of vaporization are 9% for methanol, 15% for water, and 24% for ammonia.

With this model for the liquid, the estimate of the three-body correction to the energy could be made from ab initio calculations on sequential ammonia trimers. At the minimal basis set level (STO-3G), the nonadditives of the dimer energies for optimized head-to-tail, double donor, and double acceptor trimers are −0.8, +0.4, and +0.1 kcal/mol, respectively.[19] Double ζ (4-31G) basis set calculations predict a nonadditivity of −0.5 kcal/mol for the head-to-tail trimer. The head-to-tail arrangement dominates in the polymeric chains so the energy of the liquid should be lowered by 0.5–1.0 kcal/mol if three-body effects are included.

Finally, the distributions for the hydrogen bond angles are shown in Figure 14 from the Monte Carlo calculation with the S-12-6-3-1 potential. The results with the 12-6-3-1 potential are similar. θ is the N···N–H angle and ϕ is the N···H–N angle. The potential function favors values near 0 and 180°, respectively. The maxima for the liquid occur at 25 and 167°. Thus, the average hydrogen bond is significantly bent; however, it is more appropriate in analyzing the linearity to plot the number of hydrogen bonds per unit solid angle, i.e., by dividing the distributions by sin θ and sin ϕ.[24] When this correction for the volume element is made, the preference for linearity is reaffirmed. Distributions for ϕ have been obtained from neutron-diffraction experiments on solids involving a variety of X–H···Y hydrogen bonds.[24] Interestingly, the location of the maximum and range of the distribution are the same as found here for ammonia and previously for methanol.[5b] The distributions also rule out a significant component of cyclic dimers in liquid ammonia since they would be represented by values of ϕ near 120°.

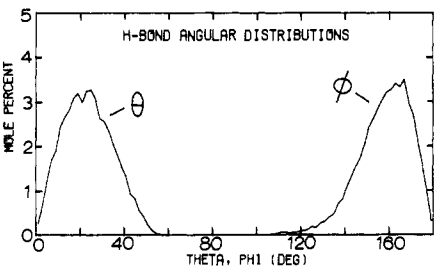

Figure 14. Distributions for the angles θ (N···NH) and ϕ (N···HN) between hydrogen-bonded monomers in liquid ammonia from the Monte Carlo simulation with the S-12-6-3-1 potential function. The units for the Y axis are mole percent per degree.

V. Conclusion

Monte Carlo statistical mechanics calculations for liquid ammonia have been reported here. From this and previous studies of water,[3e] hydrogen fluoride,[4b] and methanol,[5] it has been established that useful intermolecular potential functions can be derived from minimal basis set ab initio molecular or-

bital calculations with no or minor modifications. The results of the simulations have been thoroughly analyzed to obtain intimate descriptions of the liquids' structures. Ammonia, hydrogen fluoride, and methanol are all found to contain winding hydrogen-bonded chains with an average of two hydrogen bonds for each monomer. For ammonia, this is a significant departure from the structure of the solid. Liquid water has a more complex network with many interconnecting rings and an average of 3.5 hydrogen bonds per monomer. The combined quantum and statistical mechanics approach to modeling fluids is a powerful tool that will be most useful in studying solvent effects in organic chemistry and biochemistry.

Acknowledgments. Gratitude is expressed to the National Science Foundation (CHE-7819446), Dreyfus Foundation, and Sloan Foundation for support of our research programs. Acknowledgment is made to the donors of the Petroleum Research Fund, administered by the American Chemical Society, for support of this research. This work was also supported in part by the National Resource for Computation in Chemistry under a grant from the National Science Foundation (Grant CHE-7721305) and the Basic Energy Sciences Division of the U.S. Department of Energy (Contract No. W-7405-ENG-48). Dr. Phillip Cheeseman kindly provided the program to make the stereoplots. The authors are also grateful to Yarmouk University, Irbid, Jordan, for a fellowship granted to M.I.

References and Notes

(1) Quantum and Statistical Mechanical Studies of Liquids. 8. Part 7: ref 5b.
(2) Camille and Henry Dreyfus Foundation Teacher-Scholar, 1978–1983; Alfred P. Sloan Foundation Fellow, 1979–1981.
(3) (a) Rahman, A.; Stillinger, F. H. *J. Chem. Phys.* **1971**, *55*, 3336. Stillinger, F. H.; Rahman, A. *Ibid.* **1974**, *60*, 1545; **1978**, *68*, 666. (b) Lie, G. C.; Clementi, E.; Yoshimine, M. *Ibid.* **1976**, *64*, 2314. (c) Swaminathan, S.; Beveridge, D. L. *J. Am. Chem. Soc.* **1977**, *99*, 8392. (d) Owicki, J. C.; Scheraga, H. A. *Ibid.* **1977**, *99*, 7403. (e) Jorgensen, W. L. *Ibid.* **1979**, *101*, 2011, 2016. *Chem. Phys. Lett.*, in press.
(4) (a) Jorgensen, W. L. *J. Am. Chem. Soc.* **1978**, *100*, 7824. (b) *J. Chem. Phys.* **1979**, *70*, 5888. (c) Klein, M. L.; McDonald, I. R.; O'Shea, S. F. *Ibid.* **1978**, *69*, 63. (d) Klein, M. L.; McDonald, I. R. *Ibid.* **1979**, *71*, 298.
(5) (a) Jorgensen, W. L. *J. Chem. Phys.* **1979**, *71*, 5034. (b) *J. Am. Chem. Soc.* **1980**, *102*, 543.
(6) (a) McDonald, I. R.; Klein, M. L. *J. Chem. Phys.* **1976**, *64*, 4790. (b) McDonald, I. R.; Klein, M. L. *Discuss. Faraday Soc.* **1978**, *66*, 48. (c) Duquette, G.; Ellis, T. H.; Scoles, G.; Watts, R. O.; Klein, M. L. *J. Chem. Phys.* **1978**, *68*, 2544.
(7) Narten, A. H. *J. Chem. Phys.* **1977**, *66*, 3117; **1968**, *49*, 1692.
(8) (a) Popkie, H.; Kistenmacher, H.; Clementi, E. *J. Chem. Phys.* **1973**, *59*, 1325. (b) Matsuoka, O.; Clementi, E.; Yoshimine, M. *Ibid.* **1976**, *64*, 1351.
(9) (a) Benedict, W. S.; Plyler, E. K. *Can. J. Phys.* **1957**, *35*, 1235. (b) Kuchitsu, K.; Guillory, J. P.; Bartell, L. S. *J. Chem. Phys.* **1968**, *49*, 2488. (c) Odutola, J. A.; Dyke, D. R.; Howard, B. J.; Muenter, J. S. *Ibid.* **1979**, *70*, 4884.
(10) Hehre, W. J.; Lathan, W. A.; Ditchfield, R.; Newton, M. D.; Pople, J. A. *QCPE* **1973**, *10*, 236.
(11) Jorgensen, W. L.; Cournoyer, M. E. *J. Am. Chem. Soc.* **1978**, *100*, 4942.
(12) Dill, J. D.; Allen, L. C.; Topp, W. C.; Pople, J. A. *J. Am. Chem. Soc.* **1975**, *97*, 7220.
(13) (a) Lowder, J. E. *J. Quant. Spectrosc. Radiat. Transfer* **1970**, *10*, 1085. (b) Lambert, J. D.; Strong, E. D. T. *Proc. R. Soc. London, Ser. A* **1950**, *200*, 566.
(14) Curtiss, L. A.; Frurip, D. J.; Blander, M. *J. Chem. Phys.* **1979**, *71*, 2703.
(15) (a) Olovsson, I.; Templeton, D. H. *Acta Crystallogr.* **1959**, *12*, 832. (b) Reed, J. W.; Harris, P. M. *J. Chem. Phys.* **1961**, *35*, 1730.
(16) Nelson, R. D.; Lide, D. R.; Maryott, A. A. *Natl. Stand. Ref. Data Ser., Natl. Bur. Stand.* **1967**, *No. 10*.
(17) Jander, G. "Chemistry in Nonaqueous Ionizing Solvents", Vol. 1; Wiley-Interscience: New York, 1966.
(18) (a) Overstreet, R.; Giauque, W. F. *J. Am. Chem. Soc.* **1937**, *59*, 254. (b) Haar, L.; Gallagher, J. S. *J. Phys. Chem. Ref. Data* **1978**, *7*, 635.
(19) Jorgensen, W. L.; Ibrahim, M., unpublished results.
(20) Mezei, M.; Swaminathan, S.; Beveridge, D. L. *J. Chem. Phys.* **1979**, *71*, 3366.
(21) (a) Keyes, F. G. *J. Am. Chem. Soc.* **1938**, *60*, 1761. (b) Rowlinson, J. S. *Trans. Faraday Soc.* **1949**, *45*, 974. (c) Cottrell, T. L.; Macfarlane, I. M.; Read, A. W. *Ibid.* **1965**, *61*, 1632.
(22) Pangali, C.; Rao, M.; Berne, B. J. *Chem. Phys. Lett.* **1978**, *55*, 413.
(23) (a) Narten, A. H.; Levy, H. A. *J. Chem. Phys.* **1971**, *55*, 2263. (b) Narten, A. H. *Ibid.* **1972**, *56*, 5681.
(24) Olovsson, I.; Jönsson, P. In "The Hydrogen Bond", Schuster, P., Zundel, G., Sandorfy, C., Eds.; North-Holland Publishing Co.: Amsterdam, 1976; p 393.

Structures and Isotopic Fractionation Factors of Complexes, $A_1HA_2^-$ [1]

Maurice M. Kreevoy* and Tai Ming Liang

Contribution from the Laboratory for Chemical Dynamics, Department of Chemistry, University of Minnesota, Minneapolis, Minnesota 55455. *Received August 27, 1979*

Abstract: The isotopic fractionation factors of homo- and heteroconjugate complexes[2] are shown to reach a minimum just below 0.3 for substances in which the linear motion of the bridging hydrogen is governed by a double minimum potential function, with the lowest allowed vibrational level in the neighborhood of the central maximum. Both biphenolates and bicarboxylates generate such fractionation factors. The electronic spectra of the nitro-substituted biphenolates require that these substances be mixtures of degenerate tautomers, and, therefore, that their lowest allowed vibrational levels should fall somewhat below the central maxima in their potential functions. Crystallographic and other evidence indicates that the bridging proton in the bicarboxylates oscillates about the O···O center, so their lowest allowed vibrational levels appear to fall above the central maximum, but the fractionation factors appear to exclude single minimum potential functions. Many properties of these substances are fairly well modeled with simple, quartic-quadratic potential functions. A heteroconjugate complex is predicted and observed to have a somewhat higher fractionation factor; however, the fractionation factor should not be too elevated if the complex is not too unsymmetric. The fractionation factors of strongly unsymmetrical heteroconjugates should approach those of the uncomplexed acids (about unity). The potentials of heteroconjugates can be modeled with quartic-cubic-quadratic functions.

The structure of bicarboxylate ions and related substances, $A_1A_2H^-$,[2] has been the subject of a large number of investigations.[3-6] These investigations have attempted to distinguish compounds in which the hydrogen oscillates about a central position from those which are mixtures of degenerate or near-degenerate tautomers. In the latter case the lifetime of the individual tautomers is also of interest. In all cases the ultimate objective is to approximate the potential functions governing the motions of the bridging hydrogens. In the present paper we show that a uniquely low isotopic fractionation factor

0002-7863/80/1502-3315$01.00/0